JOURNAL OF OPTOELECTRONICS AND ADVANCED MATERIALS, Vol. 10, No. 10, October 2008, p. 2811 - 2817

Studies on multifunctional textile materials. Plasma deposition onto textile materials and onto reference plates

T. BEICA, L. C. NISTOR*, C. MOROSANU, L. FRUNZA, G. E. STAN, I. ZGURA, D. MARCOV, A. DOROGAN[a], E. CARPUS[a]
National Institute of Materials Physics, 077125 Magurele, Romania
[a]*Research-Development National Institute for Textile and Leather, 030508 Bucharest, Romania*

The magnetron sputtering method was used to obtain layers of indium tin oxide or hydroxyapatite on glass fiber woven and on reference glass plates. The layers were characterized by scanning microscopy, UV-vis spectroscopy and conductivity measurements. Hydrophilic properties of the woven samples were investigated by optical microscopy following the behavior of a water droplet upon the each of the samples. The change of the drop profile in time due to wetting of the fabric leads to the wetting kinetics. The most efficient treatments to improve the hydrophilic/wetting properties of the glass fiber woven were found.

(Received July 5, 2008; accepted August 14, 2008)

Keywords: Plasma deposition, ITO layer, Hydroxyapatite layer, Glass fiber woven, Wetting properties

1. Introduction

Various experiments have been performed in order to transform textiles into multifunctional materials For example, we attempted to obtain two effects: 1) an antistatic effect, by covering the textile with a transparent electrical conductive layer, preserving its appearance; 2) a modification of the textile hydrophobicity through the modification of the surface energy.

The magnetron sputtering (MS) method is used both in production and in research for covering substrates of practically any shape. A wide range of materials can be covered through this technique, any solid state metal, oxides, ceramics and a large variety of composites (e.g. [1]. In this paper we study the modification of the surface properties of a glass fiber woven used as model for a textile woven, covered by magnetron sputtering with different modifiers such as hydroxyapatite (HA), a ceramic material well known for its biocompatibility and bioactivity [2] and with indium tin oxide (ITO), a material transparent for visible radiation and showing remarkable properties of electrical conductivity depending on the layer thickness [3].

The deposited layers were analysed by scanning electron microscopy, UV-vis spectroscopy and conductivity measurements. In addition, the hydrophobic/hydrophilic properties of the deposited layers were studied by optical microscopy, following the behavior of a water droplet onto the deposited glass fiber woven.

2. Experimental

The woven of glass fibers (further noted GFW) is a commercial material. It has been used as received. Glass plates (further noted GP) were used as well for comparison.

The plasma deposition equipment employed a vacuum stage consisting of a preliminary vacuum pump and a diffusion pump (of ca. $2x10^{-6}$ Torr). The working gases are introduced through a three way admission system, each having needle taps and rotameters. A schematic image of the deposition chamber is presented in Figure 1.

The ITO target was prepared by mixing high purity oxide powders of indium (In_2O_3, 9%) and tin (SnO_2) while the target of HA was prepared by cold pressing HA powder in a copper crucible.

Preparation of the substrates for plasma deposition. Glass plates were cleaned in acetone and then in ethanol baths under ultrasonication; afterwards they were dried under nitrogen flow. Glass fiber woven substrates were mounted as such on the substrate holder. Inside the deposition chamber, all the samples were cleaned by etching under argon plasma.

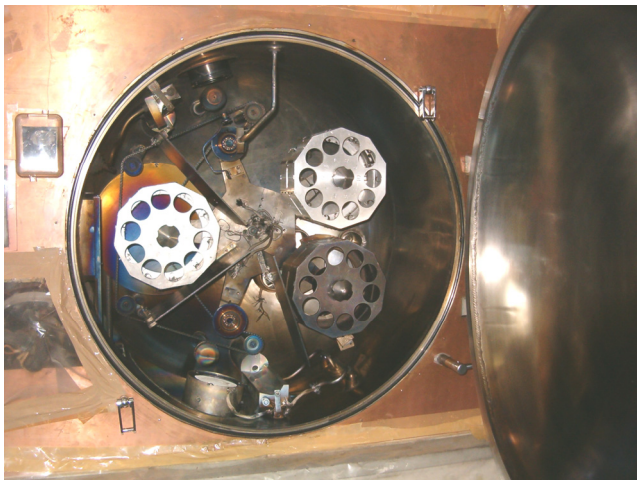

Fig. 1. An overall view of the magnetron sputtering and plasma-enhanced chemical vapour deposition chamber.

The description of the glass woven samples and their corresponding reference glass plates is given in Table 1. The sample label carries additional information related to the particular deposition conditions.

Table1. The description of the samples used in this study

Nr.	Sample name	Composition
1	HA/GP(T3/F1)	HA/Glass plate
2	HA/GFW(T3/F1)	HA/Glass fiber woven
3	ITO/GP(T5/F2)	ITO/Glass plate
4	ITO/GP(T5/F5)	ITO/Glass plate
5	ITO/GP(T5/F8)	ITO/Glass plate
6	ITO/GFW(T5/F2)	ITO/Glass fiber woven
7	ITO/GFW(T5/F5)	ITO/Glass fiber woven
8	ITO/GFW(T5/F8)	ITO/Glass fiber woven

The conditions in which the MS deposition was performed are listed in Table 2. The pressure is rather low despite some disadvantages [4] of the procedure.

Table 2. Conditions for HA and ITO depositions by magnetron sputtering

Sample	Pressure (Pa)	Flow (sccm)	Ar/O2	Time (min)	Thickness (nm)	DC bias (V)
HA/GP(T3F1)	0.24	44	100	30	310	80
ITO/GP(T5F2)	0.3	46	95/5	15	(280)	260
ITO/GP(T5F5)	0.3	46	95/5	20	(320)	258
ITO/GP(T5F8)	0.3	46	95/5	25	(400)	255

The JEOL 200 CX electron microscope used for structural characterizations can work both in transmission (TEM) and scanning (SEM) modes. For the textile fibers especially, the SEM mode was useful, as it allows the study of the morphological and topographic changes of the fibre surface exposed to various functionalizing treatments.

Preparation of the textile materials for the examination by electron microscopy. The woven samples (electrically insulating) were fixed (with a colloidal silver paste) on the sample holder in such a way to ensure the electrical contact between the sample and the metallic sample holder and then covered with a thin conductive layer (a thin copper layer deposited in vacuum) to avoid electrical charging of the sample during the observations.

Measurements by UV-vis spectroscopy were performed with a Lambda 45 Perkin Elmer spectrometer with reflectance equipment.

Properties of water droplet in contact with the deposited layers were followed by optical visualization [5, 6]. The samples were obliquely (45^o) illuminated from a white cold source. Water droplets were introduced using a syringe needle. The droplet was followed by optical microscope at 45^o the receiver being a Nikon Coolpix 2000 camera (collecting 5 images/s). For vizualisation at large angles a Commax CRC-41CP CCD camera has been used.

3. Results and discussion

Characterization by electron microscopy

Fig. 2a shows the general aspect of the woven covered with a layer of hydroxyapatite. It can be noted that the deposition is relatively uniform and covers well the woven fibers. At a higher magnification (Figure 2b) however, it can be seen that in some areas along the fiber some fine cracks appear.

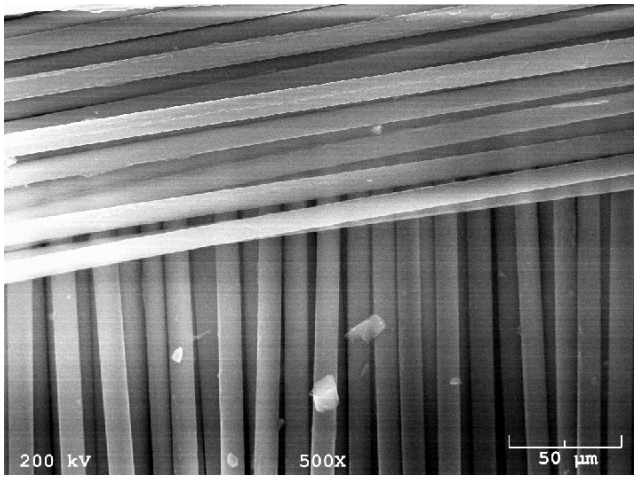

a

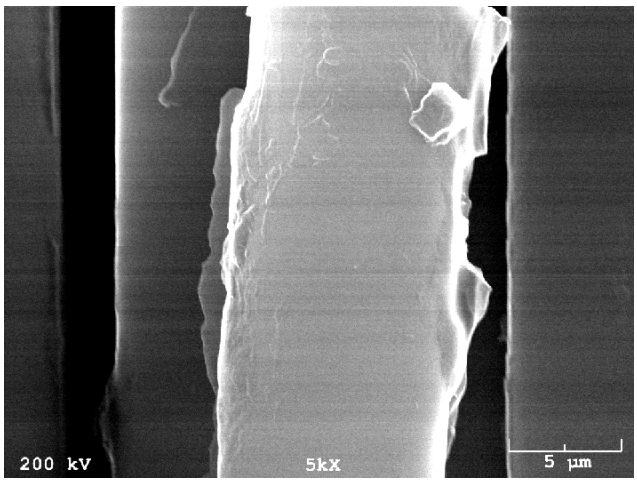

b

Fig. 2. SEM photographs of the sample HA/GFW(T3/F1) at different magnifications: a) 500X; b) 5000×.

For comparison, Fig. 3 shows the morphological aspect of the same deposition but on a glass plate. In this case the deposition is also very uniform but the fine granulation of the HA layer is more visible than in the case of the woven (both images were taken using the same magnification).

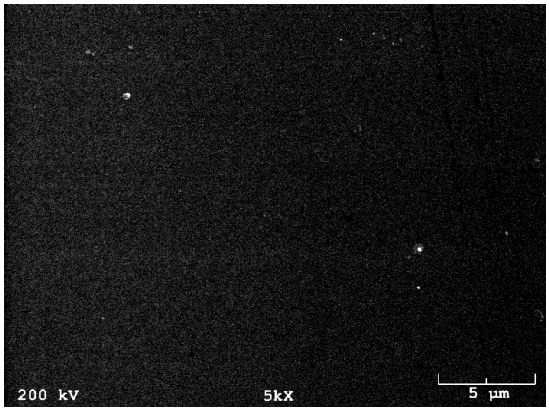

Fig. 3. SEM photographs of the sample HA/GP(T3/F1). Magnification of 5000×.

Fig. 4 gives the general aspect of the glass fiber woven with a layer of ITO.

If we compare the SEM images from Fig. 2a and 4a, which are taken at the same magnification, it can be seen that the ITO layer is less uniform than the HA layer. This morphological aspect is revealed also for larger magnifications (Fig. 4b).

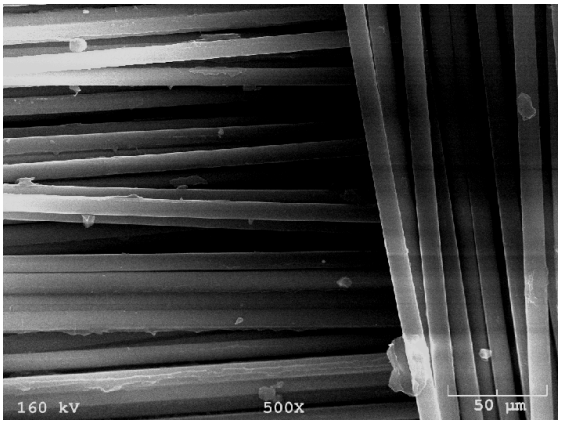

a

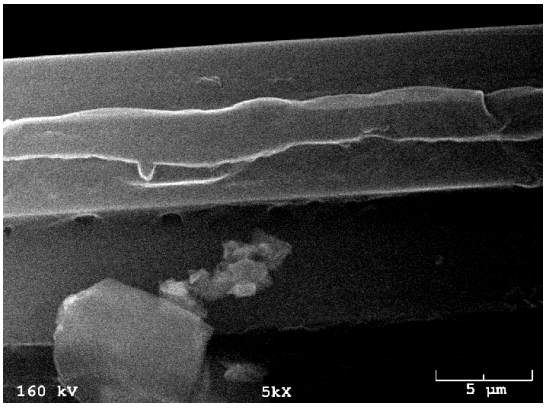

b

Fig. 4. SEM images of the sample ITO/GFW(T5/F2) at the magnification of a) 500×; b) 5000×..

SEM image from Fig. 5 shows that the ITO layer on the glass plate is no uniform. Holes can also be noted along the woven fibers deposited with ITO.

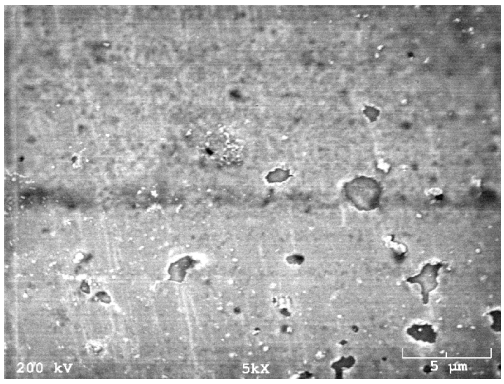

Fig. 5. SEM image of the sample ITO/GP(T5/F2) at the magnification of 5000×.

The presence of various irregularities in the ITO layer as compared to the HA layer, both deposited in the glass fiber woven might be explained by the fact that the wetting time of the woven with ITO is 3.5 times less than the wetting time of the woven with the HA (see further).

In Fig. 6 the SEM images of the ITO/GFW(T5/F5) are presented; the ITO layer, although is thicker than that of the sample ITO/GFW(T5/F2) (see Table 2) has a similar morphological aspect with irregularities and the deposition defects appearing along the woven fibers. The deposition on a planar glass substrate shows also some heterogeneity of the deposition.

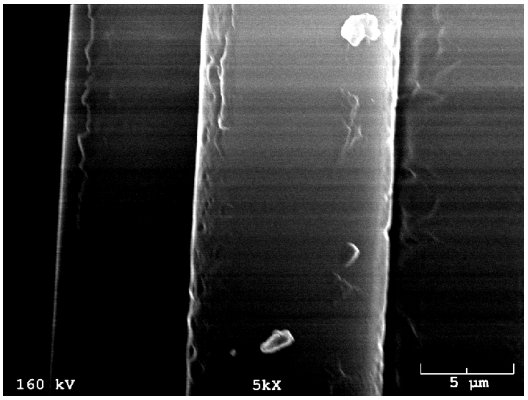

Fig. 6. SEM image of the sample ITO/GFW(T5/F5) (magnification of 5000X).

For comparison, the SEM image from Fig. 7 shows the morphological aspect of the ITO layer deposited on the corresponding glass plate. It can be seen in this case the non-uniformity of the deposition, which contains holes, which can also be observed along the glass fibers.

In the case of the thickest ITO layer of the sample ITO/GFW(T5/F8), the behavior already mentioned is not observed. As can be seen from the corresponding Figures (8 and 9), while the ITO layer on the woven fibers is very

cracked, almost exfoliating, the ITO layer on the glass plate is almost uniform. It turns out that the layers deposited on the fibers must no be thicker than certain values in order to keep their uniformity. Because the ITO layer on this (T5/F8) sample is already cracked it is not surprising that, as wetting tests have shown (see further), this sample is the most hydrophilic one.

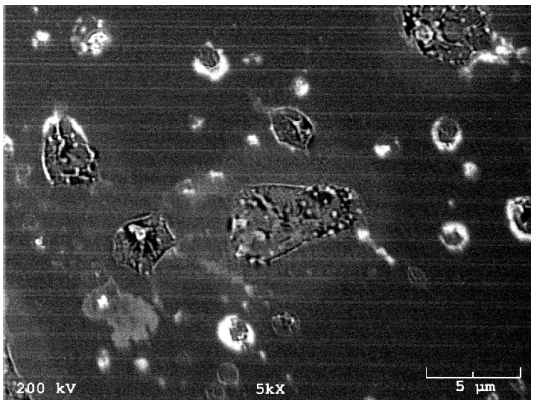

Fig. 7. SEM image of the sample ITO/GP(T5/F5) (magnification of 5000X).

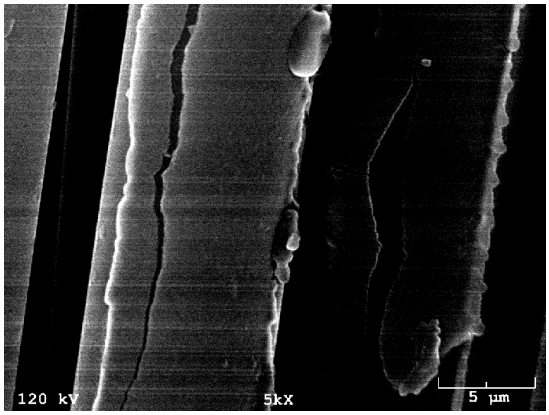

Fig. 8. SEM image at 5000× of the sample ITO/GFW(T5/F8).

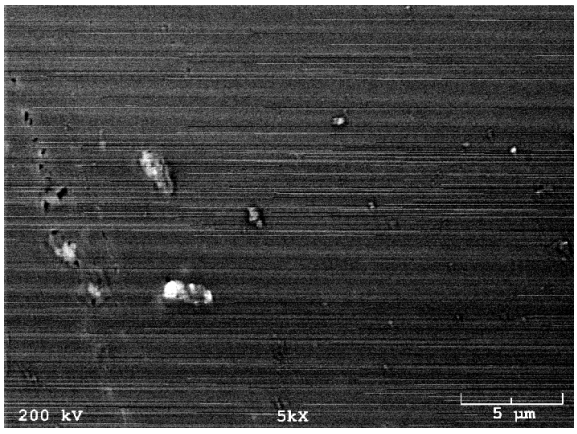

Fig. 9. SEM image at 5000× of the sample ITO/GP(T5/F8).

Optical and electrical characterization of the ITO and HA layers on glass plates.

In Fig. 10 is shown the transmission spectrum of the ITO layer deposited on glass. It can be noted a weak absorption in the range of 450÷1100 nm which clearly shows interference minima and maxima and a strong absorbance region at shorter wavelengths due to the interband absorption on the preponderant tin oxide lattice [7, 8]. From the interference region the thickness value of the layer can be calculated quite easily using the formula below

$$d = (1/2n)\,(\upsilon_1 - \upsilon_2)$$

where υ_1 and υ_2 are the wave numbers corresponding to two consecutive extreme points (minima or maxima) in the transparency region. An average value of 2.3 was used for the refractive index n of the investigated layers.

For the ITO layer whose spectrum is shown in Figure 10 the calculated thickness is d= 249 nm.

The electrical resistance of the ITO layer was measured using a digital multimeter and 1 cm separated metallic contacts placed upon the layer. Taking into consideration the thickness the estimated resistivity of the deposited layer was determined to be approximately 2 x10^{-3} (Ω.cm).

Hydrophobic properties of the layers deposited onto the glass plates

The behavior of a water droplet onto the ITO or HA layer might characterize the hydrophobic properties of these deposited layers.

Representative images of the droplet advance and wetting are given below (Figs. 11 and 12) and can lead to the determination of the corresponding angles.

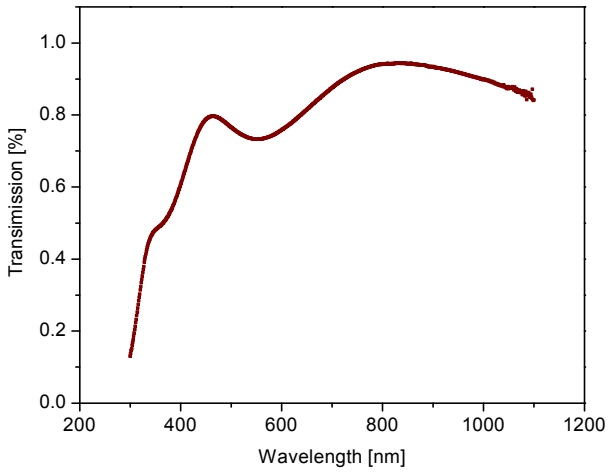

Fig. 10. Transmission spectrum of ITO layer in UV-vis range.

It results that the wetting angle depends on the surface treatment and that the advance angle is higher than the wetting one as expected. In fact, it is known that the advancing angles are below 130°, even for structures characterized by high roughness factors, unlike small-scale

structures, where values of 160-175°, were reported [9]. Besides, contact angle depends on the roughness factor, increasing with increasing the roughness.

The following relations among the samples can be established:

- advancing angle

ITO/GP(T5/F5) > ITO/GP(T5/F8)

HA/GP(T3/F1) > ITO/GP(T5/F2)

- contact angle

ITO/GP(T5/F5) < ITO/GP(T5/F8)

HA/GP(T3/F1) > ITO/GP(T5/F2)

Samples ITO/GP(T5/F8) and ITO/GP(T5/F2) have the smallest angles so that they are the most hydrophilic.

a

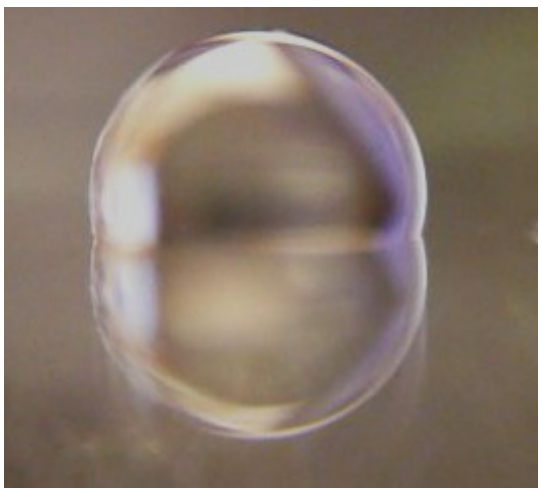

B

Fig. 11. Wetting test on a glass plate deposited with HA (sample HA/GFW(T3/F1)): a) advancing angle (~118º); b) wetting angle (~102.6º).

a

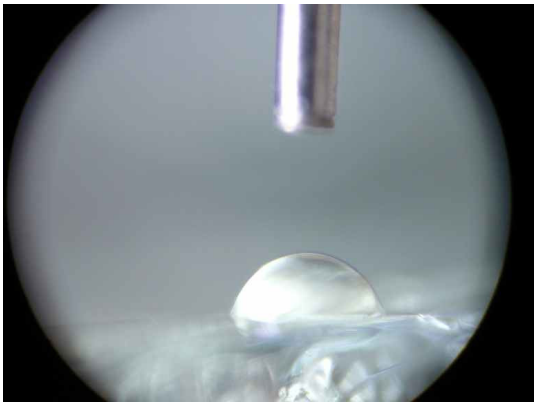

b

Fig. 12. Wetting test on a glass plate deposited with ITO (sample ITO/GFW(T3/F1)): a) advancing angle (~93º); b) wetting angle (~73º).

3.4. Hydrophobic properties of the layers deposited onto the glass fiber woven

Figs. 13-15 show the images of the water droplets onto the woven of glass fibers. Taking into consideration the times of image recording and the spot size namely the change of the drop profile in time due to wetting of the material, one can evaluate the wetting kinetics and the degree of water spreading onto the woven covered with the mentioned layers. Dried samples were obtained by exposing the samples at the room atmosphere for several hours: one can observe the formation of a persistent spot at the water contact with the woven.

We have to mention that the woven color which appears in the images is not identical to the one observed by eye because of various factors like the spectrum and polarization of light from the source, the absorption/transmission properties of the woven etc. For determining the wetting properties these factors are not of interest, at least apparently and thus they were not mentioned or monitored every time.

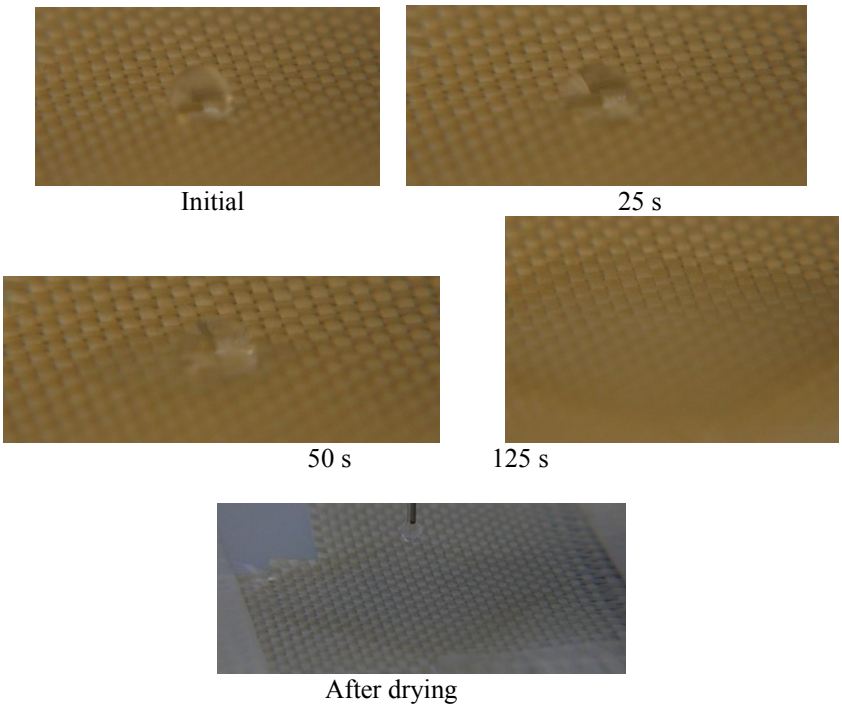

Fig. 13. Wetting test on the sample HA/GP(T3F1).

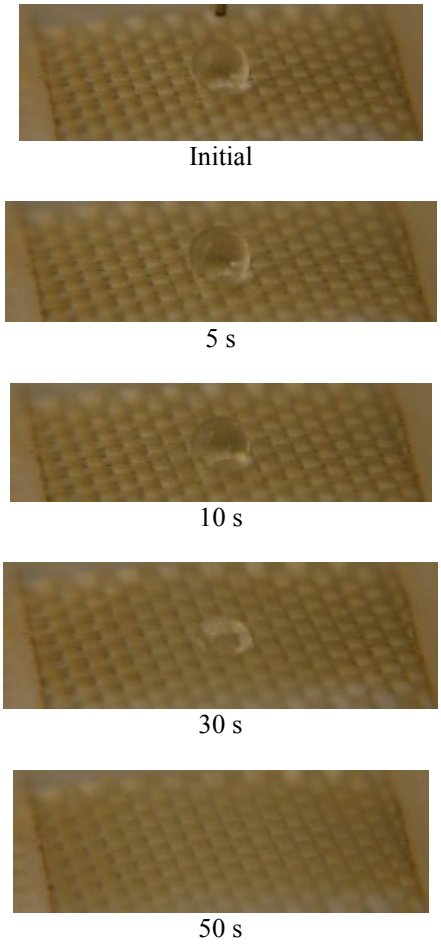

Fig. 14. Wetting test on the sample ITO/GP(T5F2).

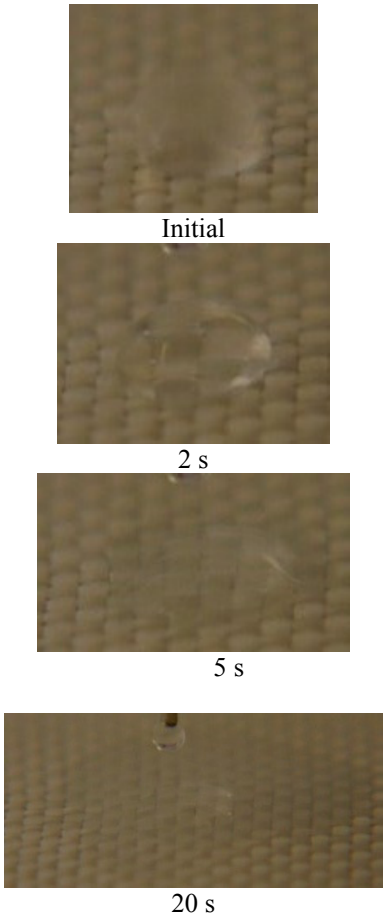

Fig. 15. Wetting test on the untreated glass fiber woven. The images are taken at the same magnification, but their size is different to follow easier the water spot.

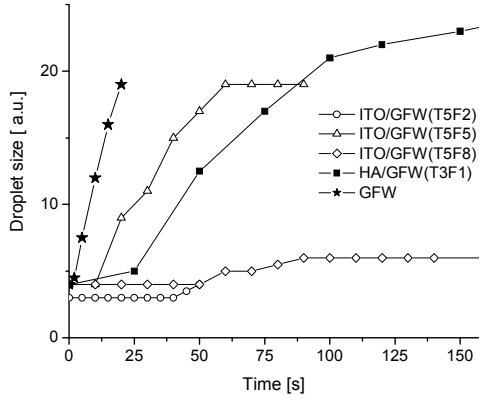

a

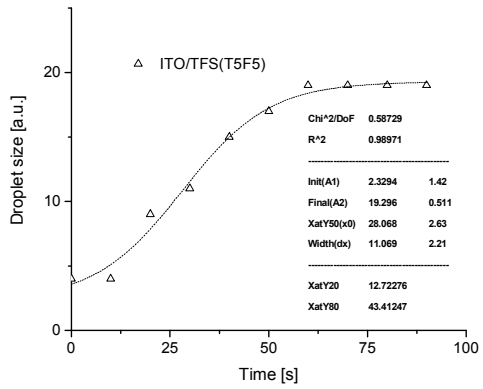

b

Fig. 16. Wetting kinetics on the samples with layers of ITO or HA. Pending droplet has ~2 units. a) Samples as shown in the legend; b) Sigmoid fit of sample ITO/GFW(T5F5).

It is obvious that the wetting is much faster on ITO/GFW(T5F2) than on HA/GFW(T3F1). The wetting sequence of remnant wetting (area that is wet by the liquid water) is thus

GFW < ITO/GFW(T5F2) < HA/GFW(T3F1).

The wetting kinetics can be followed in the Figure 16. All the curves have a sigmoid shape, as shown an example in Fig. 16b. This fact indicates a cooperative behavior. One can note also that the wetting is faster on the untreated woven than on those with ITO or HA layer. The most efficient treatment seems to be the ITO treatment under the conditions (T5F8) and (T5F2).

4. Conclusions

Layers of indium tin oxide or hydroxyapatite were deposited onto samples of glass fiber woven and on reference glass plates by magnetron sputtering method.

The layers were characterized by scanning electron microscopy, UV-vis spectroscopy and conductivity measurements.

The HA layer was rather uniformly deposited, covering well the woven fibers. However, in some areas along the fiber some fine cracks can be observed. These defects are more visible on the reference plates.

The ITO layer is less uniform than the HA layer. The thickest ITO layer on the woven fibers is very cracked, almost exfoliating, while on the glass plate is almost uniform. It turns out that the layers deposited on the fibers must not be too thick in order to preserve their uniformity.

The hydrophobic/hydrophilic properties of the woven samples were investigated by optical microscopy following the behavior in time of a water droplet upon the samples. Wetting kinetics were thus obtained showing sigmoid shapes, probably due to a cooperative behavior.
The wetting is faster on the untreated woven than on the woven with ITO or HA layer. The most efficient treatment seems to be the ITO treatment under the conditions (T5/F8) and (T/5F2) as shown in Table 2. The sample with the thickest ITO layer seems to be the most hydrophilic one.

Acknowledgements

The authors are indebted to Romanian Ministry for Research for the financial support (either under Project CEEx S2C09 MATNANTECH or under Project PN06-410102 Core Program).

References

[1] V. Dumitru, C. Morosanu, V. Sandu, A. Stoica, Thin Solid Films **359**, 17 (2000).
[2] L.C. Nistor, C. Ghica, V. S. Teodorescu, S.V. Nistor, G. Dinescu, D. Matei, N. Frangis, N. Vouroutzis, C. Liutas, Mater. Res. Bull. **39,** 2089 (2004).
[3] T. F. Stoica, M. Gartner, M. Losurdo, V. Teodorescu, M. Blanchin, T. Stoica, M. Zaharescu, Thin Solid Films **455-456,** 509 (2004).
[4] P. Stahel, V. Bursikova, J. Bursik, J. Čech, J. Janca, M. Černak, J. Optoelectron. Adv. Mater. **10**, 213 (2008).
[5] R. Moldovan, M. Tintaru, S. Frunza, T. Beica, S. Polosan, Cryst. Res. Technol. **31**, 951 (1996).
[6] T. Beica, R. Moldovan, M. Tintaru, I. Enache, S. Frunza, Cryst. Res. Technol. **39**, 151 (2004).
[7] G. Kortum, Reflectance spectroscopy: principles, methods, applications, Springer, (1969).
[8] W. W. Wendlandt, H. G. Hecht, Reflectance spectroscopy, Wiley (1966).
[9] J. Jopp, H. Gruell, R. Yerushalmi-Rozen, Langmuir **20**, 10015 (2004).

*Corresponding author: leonis@infim.ro